Retrieval of total suspended matter concentrations from high resolution WorldView-2 imagery: a case study of inland rivers

Liangliang Shi[1,2,4], Zhihua Mao[1,2] and Zheng Wang[2,3]

[1] Zhejiang University, Hangzhou, 310028, China;
[2] State Key Laboratory of Satellite Ocean Environment Dynamics, Second Institute of Oceanography, State Oceanic Administration, Hangzhou 310012, China;
[3] School of Geographic and Oceanographic Sciences, Nanjing University, Nanjing, 210023, China

[4] sll19892029@163.com

Abstract. Satellite imagery has played an important role in monitoring water quality of lakes or coastal waters presently, but scarcely been applied in inland rivers. This paper presents an attempt of feasibility to apply regression model to quantify and map the concentrations of total suspended matter (CTSM) in inland rivers which have a large scale of spatial and a high CTSM dynamic range by using high resolution satellite remote sensing data, WorldView-2. An empirical approach to quantify CTSM by integrated use of high resolution WorldView-2 multispectral data and 21 in situ CTSM measurements. Radiometric correction, geometric and atmospheric correction involved in image processing procedure is carried out for deriving the surface reflectance to correlate the CTSM and satellite data by using single-variable and multi-variable regression technique. Results of regression model show that the single near-infrared (NIR) band 8 of WorldView-2 have a relative strong relationship (R2=0.93) with CTSM. Different prediction models were developed on various combinations of WorldView-2 bands, the Akaike Information Criteria approach was used to choose the best model. The model involving band 1, 3, 5, and 8 of WorldView-2 had a best performance, whose R2 reach to 0.92, with SEE of 53.30 g/m3. The spatial distribution maps were produced by using the best multiple regression model. The results of this paper indicated that it is feasible to apply the empirical model by using high resolution satellite imagery to retrieve CTSM of inland rivers in routine monitoring of water quality.

1. Introduction

Total suspended matter (TSM) including organic and inorganic materials which plays an important role in water quality of aquatic ecosystem. The magnitude of concentrations of TSM (C_{TSM}) has a direct influence on clarity, turbidity, color and other optical properties of water column especially in coastal and inland waters[1-3]. Suspended materials serve as a carrier and storage agent of pesticides, absorbed phosphorus, nitrogen and organic compounds and can be an indicator of pollution [4]. Sediments transport also plays an important role in global carbon cycle since half of the terrestrial organic carbon exported by rivers is ultimately buried in marine sediment [5]. Therefore, it becomes an increasingly important substances of water quality monitoring along with the industrial revolution flourishing and urban expansion arising.

Traditional methods of estimating C_{TSM} take a lot of field and laboratory efforts including water sampling, filtering and dry weight measurements which are time consuming. As inland water variables are spatially heterogeneous, synoptic information can't be obtained from the above monitoring way. From this perspective, remote sensing provides a distinct and effective way in water quality management which can give spatially distributed information [6-10]. Since the 1980s, several multispectral satellites including the Coastal Zone Color Scanner (CZCS), Sea-Viewing Wide Field-of-View Sensor (SeaWiFS), Moderate Resolution Imaging Spectroradiometer (MODIS), Medium spectral Resolution Imaging Spectrometer (MERIS) and Landsat Thematic Mapper (TM), were launched to get detailed information of the earth surface. These satellite sensors were previously applied in the open ocean called Case- Ⅰ waters in which the optical property dominated by phytoplankton. However, with the development of remote sensing techniques, it has been widely used to monitor inland and coastal water quality parameters (i.e., chlorophyll-a, turbidity, total suspended matters, temperature, chromophoric dissolved organic matter) [11-14]. Many scholars have analyzed surface water quality by using satellite multispectral data and demonstrated the relationships between remote sensing reflectance and C_{TSM} [15-21]. Meanwhile, the empirical model and semi-analytical model are used most frequently in their researches. However, previous studies commonly take the medium or low resolution satellite images as the data source which are used to establish relations with in situ measurements. Since the 20th century, a lot of commercial satellite companies provide high resolution remote sensing images (i.e., IKONOS, SPOT series, WorldView series, GeoEye-1) that make it more suitable for monitoring inland waters, especially for those quite narrow rivers. [22] adopted the approach based on analytical optical model to estimate C_{TSM} taking TM and SPOT satellite data, while [23] examined and validated the retrievals of C_{TSM} and chlorophyll-a with high resolution IKONOS multispectral data. Although these high resolution satellite data could not be analyzed using specific absorption characteristics due to its broad bandwidths and relative low signal-to-noise ratio compared with medium and low spatial resolution satellite data, the advantages of high resolution make it capable of monitoring inland rivers and reservoirs due to that these water body usually has a relative small area.

Whether the high resolution satellite image WorldView-2 with a low radiometric resolution can be applied in C_{TSM} retrieval over water body of inland rivers need to answer and evaluate. The objective of this study was to (1) develop a regression model by using high resolution WorldView-2 data to quantify C_{TSM} in inland rivers in Deqing county of Zhejiang Province, China. (2) evaluate the capability of high resolution WorldView-2 to monitor the total suspended matter over a large spatial and high dynamic region. Our study may give some evidence that WorldView-2 image were capable of detecting water quality, and can provide an alternative approach to investigate the C_{TSM} in inland rivers.

2. Data collection

2.1. Study area

Deqing County is situated in the northwest part of Hangzhou, Zhejiang province, China. Several rivers flow through the city. The region of WorldView-2 image covers an area of approximately 214 km^2 from 30°28′27.83″N to 30°35′44.56″N in latitude, and 119°58′45.21″E to 120°10′0.98″E in longitude. The area of water covers one-tenth of its total area of Deqing County and the main channel of rivers and some aquaculture areas has a high C_{TSM} respectively due to the resuspension of suspended sediments caused by the shipping and aquaculture. Figure 1 shows the geographical location of the study area.

2.2. Field campaigns

A series of surface water samples were collected from the designed sampling areas in different branch on January 9 and January 10, 2014. Levels of total suspended matter from 21 locations sampled in this study area and the sites were shown in figure 1. C_{TSM} analysis were carried out using the weighting

method, following the Chinese National Standard protocols [24]. Brief procedures were as follows: 1) water samples were collected at a depth of 0.3 m and filtered immediately onto 47 mm diameter dried and pre-weighed Sartorius™ acetate fiber filters on site, meanwhile, write down the related records of filtering. 2) The filters were stored in a refrigerator which has a −20 °C temperature before laboratory measurement. The weighing principle is that the filter should repeatedly dried in a thermal infrared dryer at 40 °C more than 4 hours and weighed until the error between the last two measurements was less than 0.01 mg. As mentioned above, sampling were collected from 1/9/2014 to 1/10/2014, whereas the overpass time of the WorldView-2 satellite is 1/10/2014. To illustrate a fact that the field data can regard as a nearly contemporaneous measurements belonging to WorldView-2 image acquisition day, meteorological data was analyzed and the result show there is no rainfall records during sampling.

3. Image processing

3.1. Radiometric calibration and geometrical correction

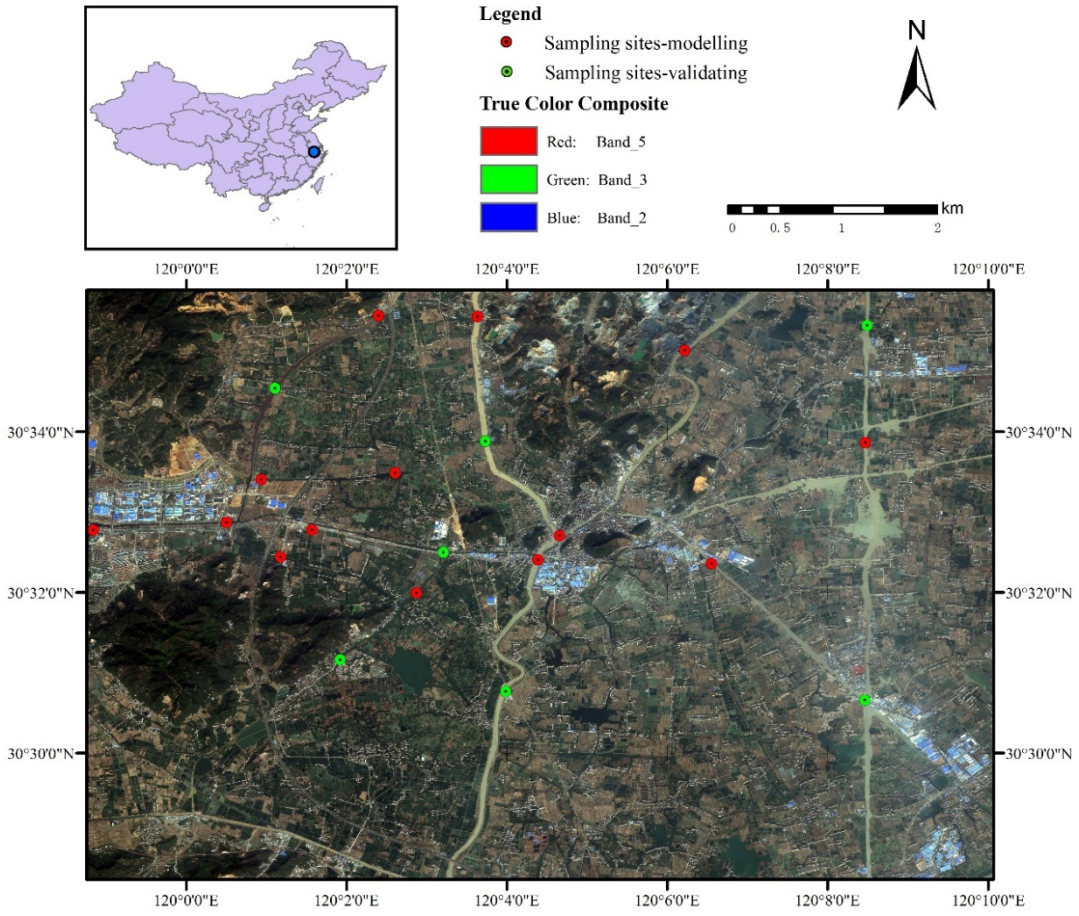

Figure 1. The study area covers the main majority part of Deqing County and field data sampling at 21 stations taken from 1/9/2014 to 1/10/2014 with acquisition of WorldView-2 satellite imagery on 1/10/2014.The red stations and blue station represent the in situ data for modelling and validation respectively. The base map is the True color composite of WorldView-2 imagery.

The satellite remotely sensed data used for this study was a high resolution WorldView-2 multispectral image acquired on January 10, 2014. Another WorldView-2 image with accurate geometric coordinates was selected as a reference image for geometric correction. WorldView-2 image has eight multispectral bands with spatial resolution of 1.8 m and swath width of 16.4 km at nadir. The detailed

characteristics of WorldView-2 bands are given in table 1. Firstly, Geometric correction was carried out after the composition of multispectral bands referred to a corrected image which was precisely geo-registered by Ground Control Points (GCPs), geometric accuracy of the image was controlled less than one pixel. The next step was radiometric correction which can convert digital numbers (DNs) to spectral radiance. The equation used for this process was as follows [25].

$$L_\lambda = \frac{DN_\lambda \cdot Calcoef_\lambda}{Bandwidth_\lambda} \quad (1)$$

where L_λ (μW/m^2/nm/sr) is the radiance for spectral band λ (nm); DN_λ is the digital value for spectral band λ ; $Calcoef_\lambda$ is the radiometric calibration coefficient; $Bandwidth_\lambda$ is the bandwidth of each spectral band at λ . $Calcoef_\lambda$ and $Bandwidth_\lambda$ of the WorldView-2 bands were reported by DigitalGlobe company and recorded in the metadata file called *.IMD, the detail calibration parameters of WorldView-2 acquired in January 10, 2014 were shown in table 2. In the study, geometric correction and radiometric calibration were operated by using corresponding module built in ENVI^{TM} 5.1 software.

Table 1. Characteristics of WorldView-2 bands.

Number	Spectral name	Wavelength(nm)	Centre wavelength(nm)	spatial resolution(m)
1	Coastal	400-450	427	1.8
2	Blue	450-510	478	1.8
3	Green	510-580	546	1.8
4	Yellow	585-625	607	1.8
5	Red	630-690	658	1.8
6	Red Edge	705-745	724	1.8
7	NIR1	770-895	832	1.8
8	NIR2	860-1040	908	1.8

3.2. Atmospheric correction

The radiance received by satellite, also known as the top of atmosphere radiance was calculated after radiometric calibration. To get the parameters of water quality from satellite imagery, the derivation of reliable spectral from satellite measurements by appropriate atmospheric correction is essential [26], several methods of atmospheric correction aimed at water bodies were developed to minimize atmospheric effects [27-32]. In this study, the Fast Line-of-Sight Atmospheric Analysis of Spectral

Table 2. Details of radiometric calibration parameters.

Number	Spectral name	Calcoef	Bandwidth
1	Coastal	9.295654e-03	4.730000e-02
2	Blue	7.291212e-03	5.430000e-02
3	Green	5.654403e-03	6.300000e-02
4	Yellow	5.101088e-03	3.740000e-02
5	Red	7.858034e-03	5.740000e-02
6	Red Edge	4.539619e-03	3.930000e-02
7	NIR1	8.726365e-03	9.890000e-02
8	NIR2	9.042234e-03	9.960000e-02

Hypercubes (FLAASH) module in ENVI was used to transform radiance image to surface reflectance image, the FLAASH method has been proved to be feasible in atmospheric correction in different multispectral medium and high resolution satellite data [33-36]. The detailed setting of parameters in

FLAASH are given in table 3, it is worth noting that the mean elevation of this study region was obtained from digital elevation model (DEM), the remaining parameters were got from the metadata file or technique documents. After running the module of atmospheric correction, water surface reflectance was obtained by eliminating the reflectance caused by the atmosphere from the calculated radiance image.

Table 3. The setting of parameters in FLAASH of WorldView-2.

Parameter name	Value	Parameter name	Value
Scene Center Location	30°32′5.78″N 120°4′25.57″	Flight Date Flight Time GMT	10,Jan,2014 2:36:58
Sensor Type	WorldView-2	Atmospheric Model	Mid-Latitude Summer
Sensor Altitude	770(km)	Aerosol Model	Urban
Ground Elevation	0.015(km)	Aerosol Retrieval	none
Pixel Size	2	Initial Visibility	30

3.3. Extracting WorldView-2 spectra

The water sampling sites shown in figure 1 were geo-located by global position system (GPS) receivers with positioning accuracy of 3 meters. All these sampling sites were later used to make relation to satellite image by recording the surface reflectance value and C_{TSM} value at the corresponding pixel. According to the previous research, it was considered better to use an average pixel value from moving window to minimize the influence of the environment around the water for high resolution data which is liable affected by random noise [23][37]. Different pixel size (window) for correlating WorldView-2 data with in-situ measurements was tested to determine the best one, a window of 5 × 5 was finally selected in this study.

3.4. Water body extraction

In order to identify water and land classes, a mask should be create to confine the satellite imagery to zone covered by water body. A decision tree classification (DTC) method which is a type of multistage classifier that can be applied to a single image or a stack of images [38] was used to distinguish the water and other terrain target. It is made up of a series of binary decisions that are used to determine the correct category for every pixel. The decisions can be based on any available characteristic of the dataset. In the study, the Normalized Difference Water Index (NDWI) was selected in the DTC module of ENVI^{TM}5.1 as a character for extracting the water body. As a result, there is a fine performance of water body extraction overall besides a slight error lies in mining region or shallow paddy fields.

4. Regression model development

Many studies have been carried out for C_{TSM} retrieval by remotely sensed data, the algorithms can be summarized as two categories: empirical model and semi-analytical model. Empirical model was established on the basis of statistical relationships between C_{TSM} and single-channel or multi-channel reflectance [19][39]. The sensitive band selection is crucial for the development of a robust model. Semi-analytical model is based on relationship between inherent optical properties (IOPs) and water components, which may combine some empirical relationships [40-41]. Due to the restrictive spectra range of WorldView-2 imagery that it can't afford the specific absorption or other characteristic of IOPs. In this study, statistical techniques have been used to derive a correlation between satellite spectral data and in situ TSM concentrations.

The existing algorithm for C_{TSM} retrieval was frequently applied in the open ocean waters or coastal waters, scarcely used in inland rivers, there are two possible reasons as follows: 1) since inland productive waters were optically more heterogeneous and complex, suspended matter may not have a dominant influence on the signal from the water surface. 2) the coverage of inland rivers were

relatively small and narrow, so the majority of satellite data can't afford an enough spatial resolution to identify the rivers, not to mention how to quantify constituents in these rivers.

Statistical techniques were adopted in our study, analyses on the Pearson correlation coefficient were developed to perform the relative strength of correction between C_{TSM} and WorldView-2 surface reflectance before building regression model. The Pearson correlation coefficients related to the sensitivity for C_{TSM} of each band were list in table 4. The results indicate that there is an increasing correlation coefficient as the wavelength increases, all the Pearson correlation coefficient of each band exceed 0.75, and the maximum value is of 0.93 appeared at wavelength of 908 nm. It is also proved that the sensitive band of total suspended matter will move to the red or NIR bands in high turbid waters [42-43]. This is because the relative high scattering from suspended matter which dominates the signal of reflectance when compared to clear waters and chlorophyll-a dominated waters.

In order to improve the accuracy of C_{TSM} retrieval, various linear regression algorithms were used to explore the best relationship between C_{TSM} and WorldView-2 satellite data, the equation can be expresses as:

Table 4. Pearson correlation coefficient between CTSM and each WorldView-2 band. WV1, WV2, WV3, WV4, WV5, WV6, WV7 and WV8 represent the reflectance of each band of WorldView-2.

	Items	**WV1**	**WV2**	**WV3**	**WV4**	**WV5**	**WV6**	**WV7**	**WV8**
C_{TSM}	Pearson Corr.	0.7678	0.7933	0.8170	0.8434	0.8574	0.8873	0.9066	0.9314
	Sig.	0.0013	0.0007	0.0004	0.0002	0.0001	0.0000	0.0000	0.0000

$$C_{TSM} = \sum A_{\lambda} \cdot WorldView-2_{\lambda} + B \quad (2)$$

where $WorldView-2_{\lambda}$ represents the atmospherically corrected reflectance in different combination of each WorldView-2 bands, A_{λ} and B are the empirical regression coefficients derived from the measurements of in situ data. In this study, the value of significance, p=0.05, was chosen to perform the statistical significance in regression analysis. Statistical Product and Service Solutions (SPSS 22.0) was used for constructing the regression models.

A first single-channel model was built using a single variable of WV8 which have the highest correlation coefficient with total suspended matter. A significant relationship (R^2=0.867, p<0.001) was observed, and the standard error of estimate (SEE) was 57.89 g/m^3.The fitted regression line and its confidence and prediction range at confidence level of 0.95 are shown in figure 2.

Different combinations of WorldView-2 bands or band ratios were used as independent variables to check which one has a better performance of C_{TSM} retrieval. The results of various regression models were shown in table 5. As for single variable model shown in figure 3, the variable WV5 lied in red band range have a relatively low relationship (R^2=0.735, SEE=81.85 g/m^3) with C_{TSM} compared to WV8 (R^2=0.867, SEE=57.89 g/m^3), the model 3 with WV1 has a weakest relationship (R^2=0.589, SEE=131.31 g/m^3), while the ratio WV8/WV1 had a higher correlation with C_{TSM}. For multi-variable models, there was a better performance than single-variable models, the strongest relationship was observed of model 7 with variables WV1, WV2, WV3 and WV8. From the regression model (model 2, model 5, model 6 and model 7) established with various variables shown in table 5, there is an obvious fact that adding variables to WV8 generally increased the R^2 values slightly. To find the best model for C_{TSM} retrieval, an evaluation rule was adopted using the Akaike Information Criteria (AIC) approach which is an estimator of the relative quality of statistical models for a given data set, the AIC values for each model are listed in table 5.

Table 5. R^2, adjusted R^2, SEE and AIC of different models.

Model	Independent variables	DF	R^2	Adj.R^2	SEE(g/m^3)	AIC
1	WV5	12	0.735	0.713	81.85	125.18
2	WV8	12	0.867	0.856	57.89	115.48
3	WV1	12	0.589	0.555	101.90	131.31
4	WV8/WV1	12	0.842	0.829	63.17	117.93
5	WV8/WV1,WV8	11	0.868	0.843	60.40	117.48
6	WV1, WV2, W8	10	0.901	0.871	54.80	115.40
7	WV1, WV2, WV3, WV8	9	0.916	0.878	53.30	115.14
8	WV2, WV3, WV5, WV8	9	0.879	0.825	63.89	120.21
9	WV5, WV6, WV7, WV8	9	0.882	0.829	63.09	119.86

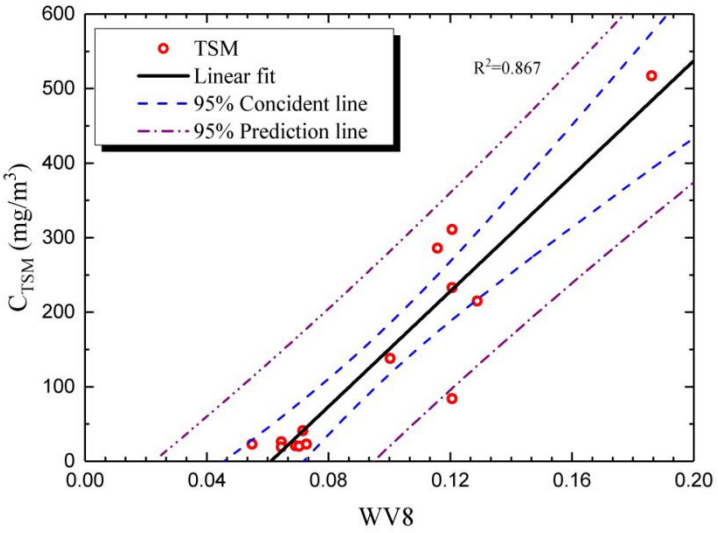

Figure 2. Single-channel model, fitted regression line between C_{TSM} and WV8 (surface reflectance of band 8), and the confidence and prediction range at the confidence of 95%.

Considering the characteristics of the regression models and the AIC value, the model 7 (R^2=0.916, AIC=115.14) which has the highest relationship and a smallest AIC value was chose as the best model for retrieving C_{TSM}. The model can express as:

$$C_{TSM} = a_1(WV1) + a_2(WV2) + a_3(WV3) + a_4(WV8) + b + \varepsilon \quad (3)$$

where WV1, WV2, WV3 and WV8 are the atmospherically corrected reflectance of WorldView-2 band, and a_1, a_2, a_3, a_4 and b are the regression coefficients of equation (3), the ε is the residuals of the model.

Since El Saadi A M [20] and Dorji P [21] established their own regression model for C_{TSM} retrieval based on WorldView-2, a comparison was made between their and our models. El Saadi A M developed the algorithm for estimating the total suspended matter using WorldView-2 data and stepwise regression model without atmospheric correction in a single branch of inland rivers, the model containing band 1, 3, 5, 6 and 7 which R^2 is of 0.39. However, in this study, band 1, 2, 3 and 8 were used to build the retrieval model after atmospheric correction which R^2 can reach to 0.916, much higher than the model built by El Saadi A M. Dorji P also developed a model based on the single band 5 of WorldView-2 over the coastal waters, and adopted the 6S (Second Simulation of a Satellite Signal in the Solar Spectrum) radiative transfer code in the atmospheric correction. However, we found that single band 8 of WorldView-2 have a best relationship with C_{TSM}, furthermore, the R^2 value of single band models is smaller than that the model using multiple bands. It is worth noting that the dynamic

range of total suspended matter in our study area is much higher than the one of El Saadi A M and Dorji P.

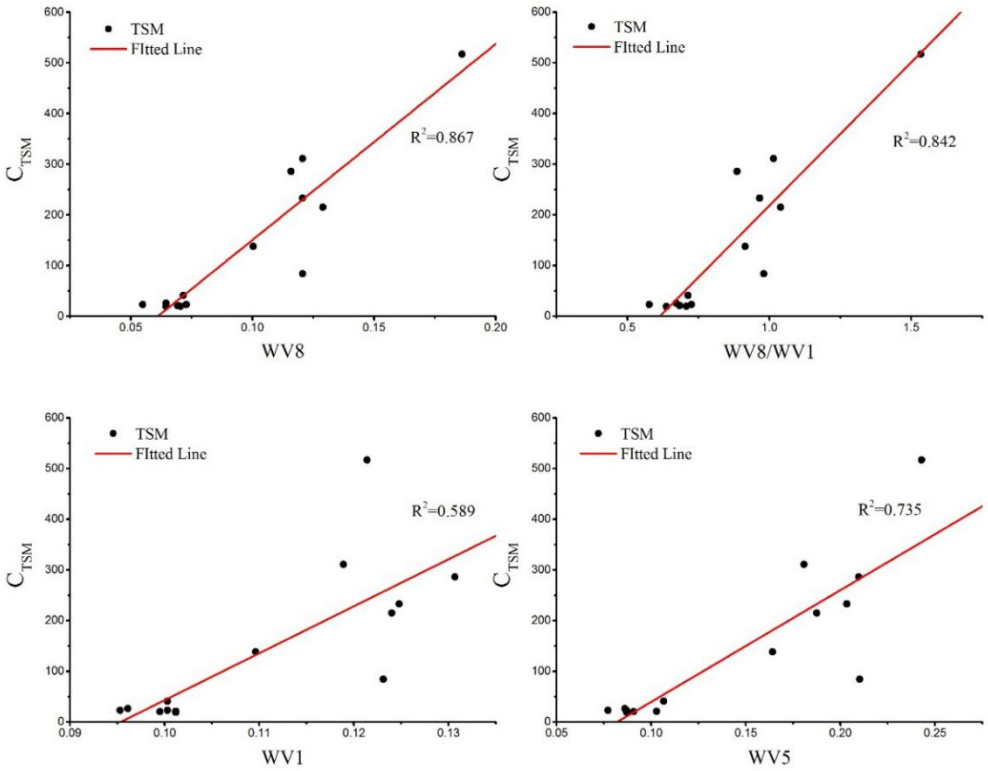

Figure 3. Retrieved results for C_{TSM} using single-channel linear regression model. WV1, WV5 and WV8 represent the surface reflectance of band 1, band 5 and band 8 of WorldView-2, respectively.

5. Validating the capability of the model

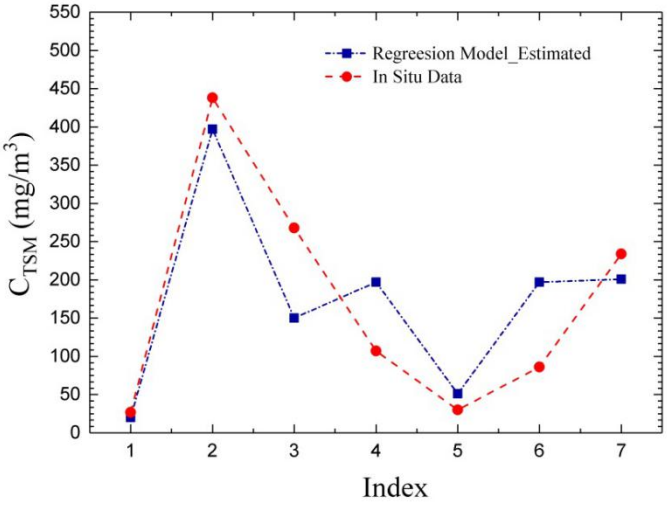

Figure 4. Comparison of the estimates by using regression model (equation 3) with in situ data. The validation data were not involved in the data for building the model.

The model for C_{TSM} retrieval is developed from the regression analysis by using statistical methods in our study. Table 5 presents the retrieved results of C_{TSM} by using multiple regression model. Among the different regression model, WV1, WV2, WV3 and WV8 were finally chosen to develop the model to predict C_{TSM}. To validate the capability of the model, we compared the model-estimated C_{TSM} derived from the equation (3) with in situ data. The validation data were not used for modelling earlier. The results were shown in figure 4, with an SEE of 62.95 g/m^3 and a mean error 63.29 g/m^3.

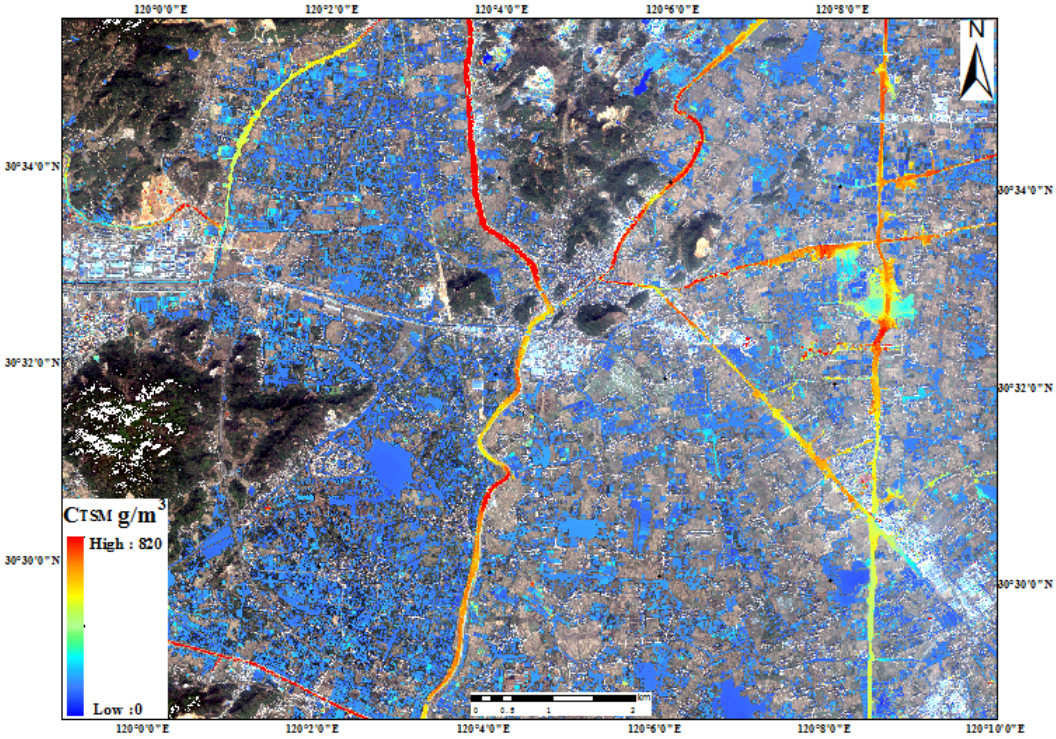

Figure 5. Distribution of C_{TSM} over the study area, the base image is 10/01/2014 dated WorldView-2 true color composited data.

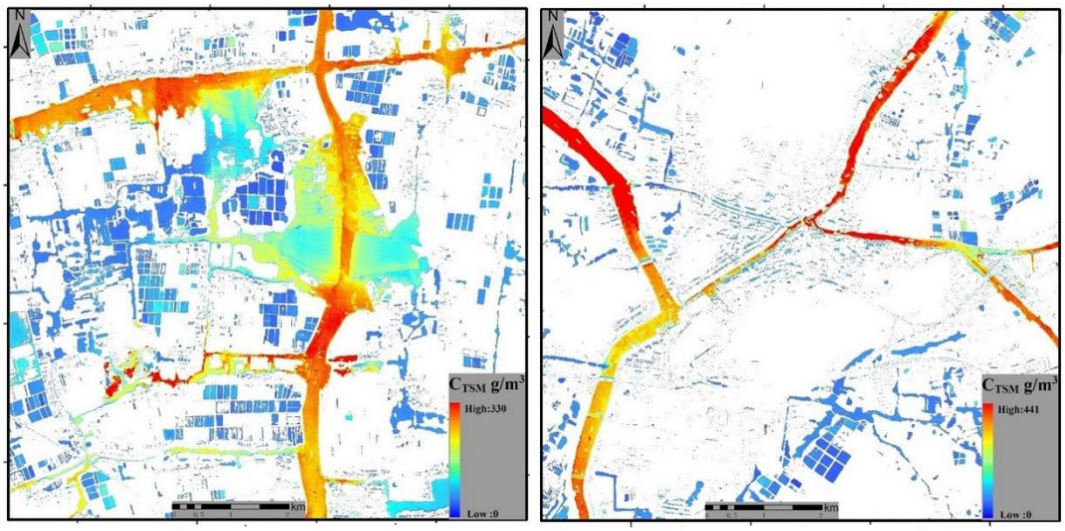

Figure 6. Distribution of TSM concentrations in fishing breading areas and shipping routes.

6. Mapping the TSM concentrations

The regression model of equation (3) was used for mapping the C_{TSM} by taking WorldView-2 remote sensing data as inputs. Figure 5 presents the spatial distribution of total suspended matter concentration over the study region. The results indicate that C_{TSM} in fishing breading areas and shipping routes is higher than other region. The likely cause of this phenomenon was that fine particles can resuspend from the bottom to the surface due to influence of roiling by fish and disturbing by boats. Figure 6 shows the two representative areas, respectively.

From the statistical perspective of C_{TSM} in the study area, On the whole, the C_{TSM} in northern zone is higher than these in southern part, while, the maximum value of the TSM concentration is 820 g/m^3, with the standard deviation is of 36.61 g/m^3. It should be noted that the C_{TSM} of pond or paddy field colored with blue in the figure 5 may partly retrieved incorrectly, due to the bottom reflectance from water surface may dominate the signal of WorldView-2 satellite imagery.

7. Conclusions

In this study, C_{TSM} retrieval in inland rivers from high resolution WorldView-2 multispectral imagery by multiple regression were demonstrated as a case study, the results give some evidence that high resolution satellite data can be applied in monitoring the water quality parameters, and give valuable information to analyze water quality variations over inland rivers. The technique used in this paper can provide an alternative approach to investigate C_{TSM} in inland waters

Despite the restrictive spectral range of multispectral WorldView-2 imagery, the sensitive analysis of each band in WorldView-2 is carried out. The results show that the sensitive band of WorldView-2 to TSM concentrations is appeared in red and near infrared band range which is consistent with the previous research, and the highest Pearson coefficient lied in WV8 (R=0.93).This provides a feasibility for the establishment of regression model between satellite remotely sensed data and in situ measurements.

Since the regression models have been the most commonly used approach to derive the TSM concentrations, the regression model for C_{TSM} retrieval was built based on reflectance of WorldView-2 and in situ C_{TSM} data. Eight regression models with various variables were constructed in this paper and results show that the multiple regression model with four independent variables (WV1, WV2, WV3 and WV8) exhibits a best performance(R^2=0.916, SEE=53.30 g/m^3). The linearity verified between the reflectance and TSM concentrations and the precision of all tested methodologies could be related to the atmospheric correction and calibration procedure.

Although the regression models established in the paper are regional algorithms, the whole procedure and methods for C_{TSM} retrieval might be extended to other regions and analyze the spatial pattern of TSM in other turbid waters. Future study is needed to collect more in situ data (including C_{TSM} and bio-optical data) to try to map the C_{TSM} distribution using other retrieval algorithms to make a comparison, such as neural network or semi-analytical approaches.

References

[1] Kirk J T O 1994 Light and photosynthesis in aquatic ecosystems *Cambridge university press*
[2] Warrick J A 2003 Short-term (1997-2000) and long-term (1928-2000) observations of river water and sediment discharge to the Santa Barbara Channel, California
[3] Ouillon S, Douillet P, Petrenko A, et al 2008 Optical algorithms at satellite wavelengths for total suspended matter in tropical coastal waters *Sensors* **8(7)** 4165-4185
[4] Jensen J R 2000 An earth resource perspective *Remote Sensing of the Environment* **72** 361-365
[5] Schlünz B, Schneider R R 2000 Transport of terrestrial organic carbon to the oceans by rivers: re-estimating flux-and burial rates *International Journal of Earth Sciences* **88(4)** 599-606
[6] Petus C, Chust G, Gohin F, et al 2010 Estimating turbidity and total suspended matter in the Adour River plume (South Bay of Biscay) using MODIS 250-m imagery *Continental Shelf Research* **30(5)** 379-392
[7] Zhou W, Wang S, Zhou Y, et al 2006 Mapping the concentrations of total suspended matter in

Lake Taihu, China, using Landsat‐5 TM data *International Journal of Remote Sensing* **27(6)** 1177-1191
[8] Sharaf El Din, E., Zhang Y, & Suliman, A 2017 Mapping concentrations of surface water quality parameters using a novel remote sensing and artificial intelligence framework *International Journal of Remote Sensing (IJRS)* **38 (4)** 1023-1042
[9] Sharaf El Din, E., & Zhang, Y 2017 Estimation of Both Optical and Nonoptical Surface Water Quality Parameters using Landsat 8 OLI Imagery and Statistical Techniques. *Journal of Applied Remote Sensing (JARS)* **11(4)** 046008
[10] Sharaf El Din, E., & Zhang, Y 2017 Improving the Accuracy of Extracting Surface Water Quality Levels (SWQLs) Using Remote Sensing and Artificial Neural Network: A Cse Study in the Saint John River, Canada Int. Arch. Photogramm. Remote Sens. Spatial Inf. Sci. XLII-4/W4 245-249
[11] Blondeau-Patissier D, Gower J F R, Dekker A G, et al 2014 A review of ocean color remote sensing methods and statistical techniques for the detection, mapping and analysis of phytoplankton blooms in coastal and open oceans *Progress in oceanography* **123** 123-144
[12] Nazeer M, Nichol J E 2015 Combining landsat TM/ETM+ and HJ-1 A/B CCD sensors for monitoring coastal water quality in Hong Kong *IEEE Geoscience and Remote Sensing Letters* **12(9)** 1898-1902
[13] Rozenstein O, Qin Z, Derimian Y, et al 2014 Derivation of land surface temperature for Landsat-8 TIRS using a split window algorithm *Sensors* **14(4)** 5768-5780
[14] Zhu W, Yu Q, Tian Y Q, et al 2014 An assessment of remote sensing algorithms for colored dissolved organic matter in complex freshwater environments *Remote Sensing of Environment* **140** 766-778
[15] Amos C L, Topliss B J 1985 Discrimination of suspended particulate matter in the Bay of Fundy using the Nimbus 7 Coastal Zone Color Scanner *Canadian Journal of Remote Sensing* **11(1)** 85-92
[16] Richter R 1990 A fast atmospheric correction algorithm applied to Landsat TM images *International Journal of Remote Sensing* **11(1)** 159-166
[17] Bilge F, Dogeroglu T, Ayday C 1999 Mapping of water quality parameters by using Landsat images in Porsuk Dam Lake, Eskisehir, Turkey//Yilmazer I *Proceedings of the International Symposium on Geology and Environment*, Istanbul, Turkey 101-107
[18] Miller R L, McKee B A 2004 Using MODIS Terra 250 m imagery to map concentrations of total suspended matter in coastal waters *Remote sensing of Environment* **93(1)** 259-266
[19] Chen Z, Hu C, Muller-Karger F 2007 Monitoring turbidity in Tampa Bay using MODIS/Aqua 250-m imagery. *Remote sensing of Environment* **109(2)** 207-220
[20] El Saadi A M, Yousry M M, Jahin H S 2014 Statistical estimation of rosetta branch water quality using multi-spectral data *Water Science* **28(1)** 18-30
[21] Dorji P, Fearns P 2017 Impact of the spatial resolution of satellite remote sensing sensors in the quantification of total suspended sediment concentration: A case study in turbid waters of Northern Western Australia *PloS one* **12(4)** e0175042
[22] Dekker A G, Vos R J, Peters S W M 2002 Analytical algorithms for lake water TSM estimation for retrospective analyses of TM and SPOT sensor data *International Journal of Remote Sensing* **23(1)** 15-35
[23] Ekercin S 2007 Water quality retrievals from high resolution IKONOS multispectral imagery: A case study in Istanbul, Turkey *Water, Air, and Soil Pollution* **183(1-4)** 239-251
[24] SAC 2007 Specifications for oceanographic survey-part 8: Marine geology and geophysics survey GB/T 12763.8-2007 *Standards Press of China*
[25] Updike T, Comp C 2010 Radiometric use of WorldView-2 imagery *Technical Note* 1-17
[26] Hu C, Chen Z, Clayton T D, et al 2004 Assessment of estuarine water-quality indicators using MODIS medium-resolution bands: Initial results from Tampa Bay, FL *Remote Sensing of Environment* **93(3)** 423-441

[27] Gordon H R, Clark D K 1981 Clear water radiances for atmospheric correction of coastal zone color scanner imagery *Applied Optics* **20(24)** 4175-4180
[28] Ritchie J C, Cooper C M, Schiebe F R 1990 The relationship of MSS and TM digital data with suspended sediments, chlorophyll, and temperature in Moon Lake, Mississippi *Remote Sensing of environment* **33(2)** 137-148
[29] Chavez P S 1996 Image-based atmospheric corrections-revisited and improved *Photogrammetric engineering and remote sensing* **62(9)** 1025-1035
[30] Ruddick K G, Ovidio F, Rijkeboer M 2000 Atmospheric correction of SeaWiFS imagery for turbid coastal and inland waters Applied optics **39(6)** 897-912
[31] Wang M, Shi W 2007 The NIR-SWIR combined atmospheric correction approach for MODIS ocean color data processing *Optics Express* **15(24)** 15722-15733
[32] Nazeer M, Nichol J E, Yung Y K 2014 Evaluation of atmospheric correction models and Landsat surface reflectance product in an urban coastal environment *International journal of remote sensing* **35(16)** 6271-6291
[33] Guo Y, Zeng F 2012 Atmospheric correction comparison of SPOT-5 image based on model FLAASH and model QUAC *International Archives of the Photogrammetry, Remote Sensing and Spatial Information Sciences* **39(7)**
[34] LUO C L, CHEN J, LE T C 2008 Atmospheric Correction on Landsat ETM+ Satellite Image Based on FLAASH Model *Protection Forest Science and Technology* **5** 46-48
[35] CHEN J, HE C, YUE C 2011 Atmospheric correction of an advance land imager (ALI) image based on the FLAASH module *Journal of Zhejiang A & F University* **4**
[36] Yu LIU 2013 Atmospheric Correction on MODIS1B Satellite Image Based on FLAASH Model *Geomatics & Spatial Information Technology* **3** 016
[37] Brivio P A, Giardino C, Zilioli E 2001 Determination of chlorophyll concentration changes in Lake Garda using an image-based radiative transfer code for Landsat TM images *International Journal of Remote Sensing* **22(2-3)** 487-502
[38] Dobra A 2009 Decision Tree Classification//*Encyclopedia of Database Systems Springer US* 765-769
[39] Tassan S 1993 An improved in-water algorithm for the determination of chlorophyll and suspended sediment concentration from Thematic Mapper data in coastal waters *International Journal of Remote Sensing* **14(6)** 1221-1229
[40] Dekker A G, Vos R J, Peters S W M 2001 Comparison of remote sensing data, model results and in situ data for total suspended matter (TSM) in the southern Frisian lakes *Science of the Total Environment* **268(1)** 197-214
[41] Zhang B, Li J, Shen Q, et al 2008 A bio-optical model based method of estimating total suspended matter of Lake Taihu from near-infrared remote sensing reflectance *Environmental Monitoring and Assessment* **145(1-3)** 339-347
[42] Doxaran D, Froidefond J M, Lavender S, et al 2002 Spectral signature of highly turbid waters: Application with SPOT data to quantify suspended particulate matter concentrations *Remote sensing of Environment* **81(1)** 149-161
[43] Nechad B, Ruddick K G, Park Y 2010 Calibration and validation of a generic multisensor algorithm for mapping of total suspended matter in turbid waters *Remote Sensing of Environment* **114(4)** 854-866